Silicon (2021) 13:1907–1915
https://doi.org/10.1007/s12633-020-00577-0

ORIGINAL PAPER

Tunable Terahertz Dielectric Resonator Antenna

Gaurav Varshney[1]

Received: 19 March 2020 / Accepted: 26 June 2020 / Published online: 12 July 2020

Abstract
An annular dielectric resonator (DR) antenna (DRA) is implemented for THz applications. A silicon made DR is loaded with graphene disk for obtaining the tunability in the frequency response. The physical parameters of silicon annular DR can be set to obtain the resonance at any frequency in the lower THz band and can be tuned by changing the chemical potential of graphene nano-disk placed at the top of the DR. The response of antenna is preserved after changing the chemical potential of graphene. The higher order hybrid electromagnetic mode is excited in the antenna structure. The proposed research work provides a way to implement the antenna for THz frequency with high gain around 3.8 dBi and radiation efficiency in the range 72 − 75%.

Keywords Silicon · Dielectric resonator · Antenna · Graphene · Disk · Chemical potential · Tuning

1 Introduction

In the recent years, wireless communication systems are being developed considering the THz band in the applications [1]. The advantage of THz spectrum is its capability in offering the wide bandwidth and hence the high data transfer rate. An antenna is always an integral part of any wireless communication system. Several antennas have been implemented for THz spectrum. In concise manner, THz antennas can be categorized into three ways; (1) the antenna with metal/dielectric radiator [2–11], (2) antenna with the radiator of 2D material [12–26], and (3) with the interface of metal/dielectric/graphene [27–34]. The first type of THz antennas can be sub categorized into two parts, one with the metallic radiator and second with dielectric radiator. In the case of metallic radiators, the surface wave and conductor losses are high at the THz frequency hence they become less efficient and they provide the efficiency around 50% [6, 8]. However, some metallic antennas were implemented providing the radiation efficiency around 80% [4, 5]. Still, the use of metal at THz frequency may be complex in practical due to their reduced conductivity [35]. The antennas implemented using the dielectric material as radiator always remains in advantage of providing the high gain and radiation efficiency [2, 11]. However, the dielectric resonator antennas (DRAs) were implemented at the higher THz spectrum falling in the optical regime. No DRA was implanted for the lower THz spectrum. Apart from these antennas, the techniques were implemented for the enhancement of gain, radiation efficiency and other performance parameters of the metal-dielectric based antennas like use of photonic crystal and frequency selective surface [10], Yagi-Uda structure with defected ground structure [9] and metamaterial cavity with reflector structure [7]. However, these improvement techniques offer complexity in terms of fabrication and size, which remains the main issue at the THz spectrum. In view of the fact that the performance parameters of THz antennas implemented using the metal/dielectric interface and radiators can be improved but still there is one limitation i.e. non-reconfigurability of their response. Industries are seeking the solution for the implementation of tunable and reconfigurable devices at micro/nanoscale. At the microwave frequency, it is possible to refabricate the devices, but it becomes a difficult task at the THz spectrum due to small scale implementations. Also, it is easy to utilize varactor or PIN diode for obtaining the tunability in the microwave devices [36]. This is a difficult task to fabricate the micro/nanoscale devices with such incorporations.

At the micro/nanoscale, the material based tunability is being explored and recently 2D material like graphene is investigated which provides the solution to the problem of non-reconfigurability [37]. Currently, researchers are on the way of numerical investigations on this novel material-based

✉ Gaurav Varshney
gauravnitd@outlook.com

[1] ECE Department, National Institute of Technology, Patna 800005, India

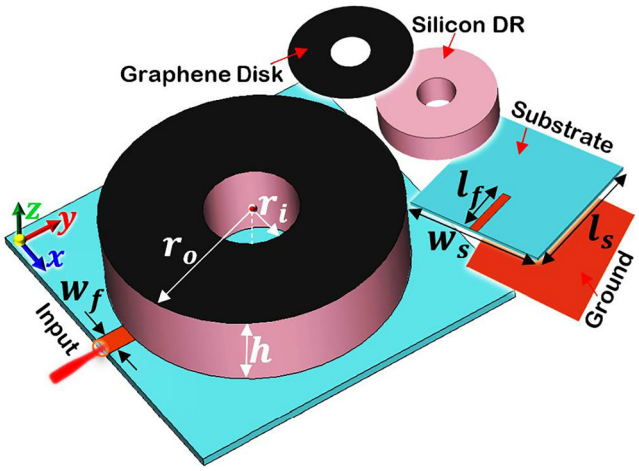

Fig. 1 The geometry of the proposed silicon DR based tunable DRA ($r_i = 8$, $r_o = 25$, $h = 13.4$, $w_f = 2.8$, $l_f = 23$, $w_s = l_s = 60$)

device which is expectedly going to become a future of the technology. In the current electronic and optoelectronics, problems are being investigated through the implementation of the devices by utilizing the graphene material [38–40]. Specially, graphene based functioning gives a thrust due to its electrical tunability with the applied external electrostatic or magnetostatics biasing [41]. The electrical tunability of material properties confers the reconfigurability in response of devices. Considering the advantages of the graphene material, the antennas have been implemented by utilizing it that comes under the second and third categories of the THz antennas. The second category of antenna utilizes the radiator made up of the graphene material [14, 19–21]. The antenna with graphene based radiator provides the reconfigurability in different performance parameters like frequency response and radiation pattern [42, 43]. The limitation of these antennas is their low radiation efficiency and gain [12, 13, 18, 25, 26]. A Y-shaped graphene antenna was reported with 24% efficiency and 0.13 dBi gain. A 26% of radiation efficiency was obtained by graphene nano-ribbon based antenna [26] which is then improved to 44% with the gain of 2 dBi [25]. A multi layered graphene patch antenna and array was also reported to provide the efficiency around 45% [12, 13]. Somehow, the efficiency of graphene antennas was improved up to 90% by using the multilayer stacked structure of graphene [21]. However, obtaining the tunability in the frequency response with multi-layered structure practically becomes a complex task [21, 44]. Also, the high gain and radiation efficiency was obtained by introducing a dielectric cavity in the graphene dipole antenna [24]. In this case, it is necessary to couple the resonance of graphene radiator with the dielectric cavity so that proper functioning can be obtained which becomes a complex task at the design level. Thus, the THz antenna of second category can provide the reconfigurability but their performance is poor.

The problems associated with the antennas of first and second category are rectified by third category. In the third category, the THz antennas were implemented with the utilization of main radiating element made up of metal and the graphene material is introduced so that the reconfigurability in response can be obtained [27, 45]. In these antennas, resonance of graphene is not a matter, it is only used for obtaining the reconfigurability in the frequency response of the metal-based radiator [29, 30]. A metallic ring antenna was implemented with graphene for obtaining the reconfigurability [29]. This antenna provides the gain around 1 dBi. The radiation efficiency of the graphene antenna was improved by utilizing the metamaterial cells up to 60% [30]. A Yagi antenna was implemented with graphene for providing the reconfigurability in the frequency response and the gain around 8.24 dBi. A microstrip patch was reported with superstrate and graphene load that drastically improves the gain up to 11 dBi and provides the 78% radiation efficiency but this acquires a large size. In the sequence, a metallic ultra-wideband antenna with graphene ribbons was implemented with the tunable dual-band notch and provides the gain and radiation efficiency 6.3 and 80%, respectively [27].

The analysis of THz antennas reveals that it is still required to implement antenna which can be fabricated in an easy way in the future. Also desired performance parameters can be obtained. The main concern of THz antennas is their low gain and radiation efficiency. This enforces the exploring of suitable way for the implementation of THz antennas. In the way to find the solution for low gain and radiation efficiency, one can think about the implementation of a dielectric resonator (DR) antenna (DRA) for THz spectrum. The DRAs are

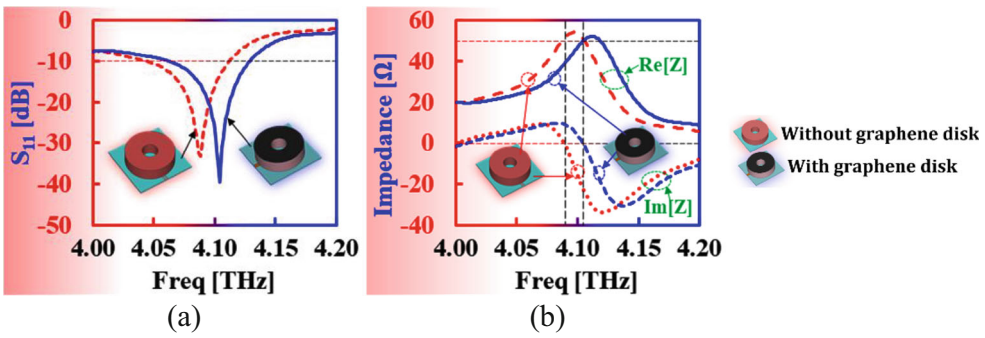

Fig. 2 The frequency response of **a** S_{11}-parameter and **b** impedance of antenna ($\mu_c = 0\ eV$, $T = 300K$, $\tau = 1\ ps$)

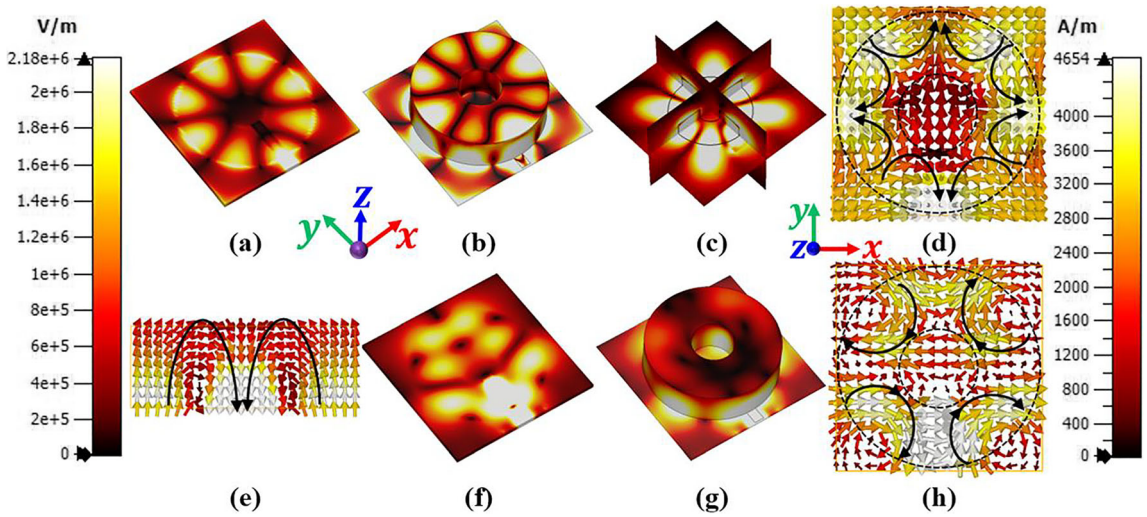

Fig. 3 *E*−field distribution in the DR with graphene disk at its top in **a** $z = 0$, **b** $z = h$, **c** in different cross-sections, **d** $z = h$ and **e** $x, y = \pm r_o$ plane and *H*−field distribution in **f** $z = 0$, **g** and **h** $z = h$ plane at frequency 4.104 THz

prominent since last three decades in microwave frequency regime since last three decades due to their capability in providing high gain and radiation efficiency and wide bandwidth [46, 47]. Also, the optical DRAs have been implemented for the same purpose [2, 11, 48]. The use of high permittivity material not only reduces size of the antenna but provides the enhanced performance also [49]. In the similar manner, the DRA can also be implemented for operating in $0.1 - 10$ THz band. Following the properties of graphene, the DRA can be coupled with the non-resonant graphene material so that tunability can be obtained. Earlier, the graphene antenna was coupled to dielectric cavity for improving the performance of the graphene antenna [24].

Following the motivation obtained from the above discussion, a DRA is implemented for THz spectrum by utilizing the silicon made DR. The utilization of silicon material provides the high permittivity which can enhance the radiation properties like gain and radiation efficiency [11]. Also, this is abundantly available which can ease the fabrication. The DRA is loaded with a graphene disk at its top surface for obtaining the reconfigurability in the frequency response by changing the chemical potential of graphene. The research issues dictating the problem of low gain and radiation efficiency with tunability of frequency response of THz antenna can be solved by utilizing the DR interfaced with graphene material. The implemented antenna provides the gain around 3.8 dBi and radiation efficiency more than 72%. Thus, the proposed antenna can replace many others implemented for THz applications. Furthermore, a tunable THz antenna array can also be implemented in the future for improving the performance parameters by utilizing the proposed single unit of tunable DRA. Moreover, this is the first research work reporting a tunable DRA for THz applications with the help of graphene material.

2 Antenna Design

Figure 1 shows the antenna structure containing a substrate made of silicon dioxide ($\epsilon_s = 3.8$) placed at the top of the conducting ground plane. A silicon DR ($\epsilon_s = 11.9$) is placed at the top of the substrate having thickness 1.6 μm. The dispersive profile of silicon material is considered as constant over the operating frequency band. Initially the dimensions of DR are selected to operate with the fundamental hybrid electromagnetic mode using the formulae given in Eq. (1) [2]. After that, the dimensions have been optimized for obtaining the desired response.

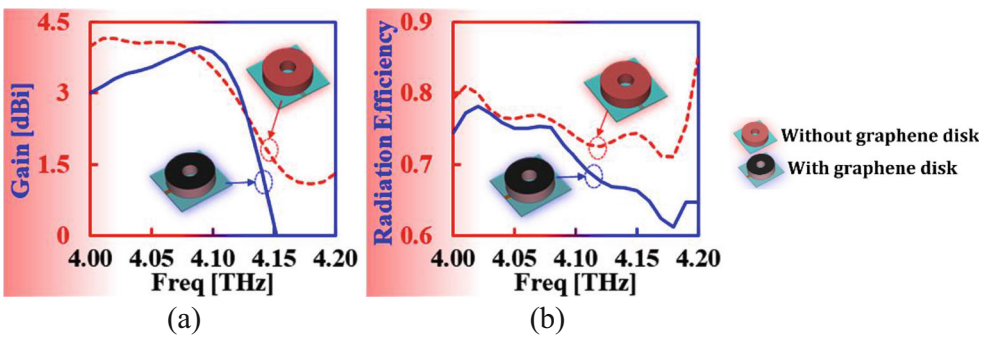

Fig. 4 **a** Gain and **b** radiation efficiency of antenna over frequency

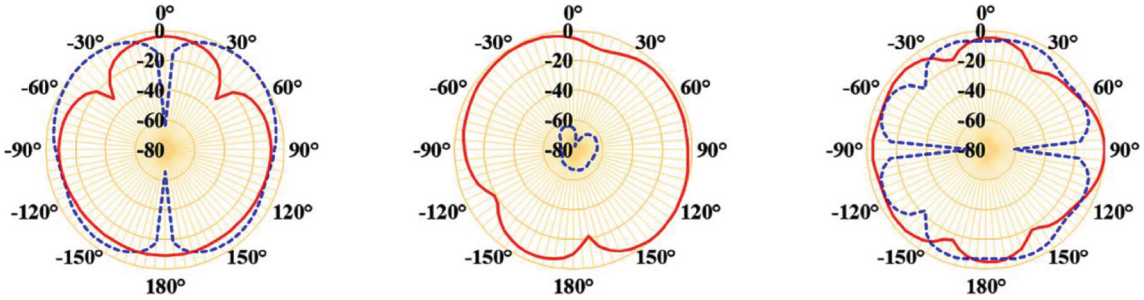

Fig. 5 Radiation pattern of tunable DRA at frequency 4.104 THz in **a** *xz*, **b** *yz* and **c** *xy*–plane (solid line-co- and dotted line- cross-polarized components of radiated field)

$$f_{vpm} = \frac{6.324c}{4r_o\pi\sqrt{\epsilon_r + 2}}\left[0.27 + 0.36\left(\frac{r_o}{h}\right) + 0.002\left(\frac{r_o}{h}\right)^2\right] \quad (1)$$

Here, *v*, *p* and *m* are integers which represent the variation of field in terms of half-wavelength along the azimuth, radius, and height of the DR [50]. Here, the DR with zero inner radius provides the resonance of fundamental hybrid mode with the selected dimensions. The excitation of any mode in the DR depends upon its aspect ratio as well as the applied feeding technique [46]. The DR of optimized dimensions provides the resonance at frequency 4.088 THz with the field distribution of the higher order hybrid mode. The selected antenna parameters with the applied feeding suppress the lower order modes. The excitation is applied to DR by using a nanostrip line made of silver material. The selection of material properties at THz frequency band becomes important in terms of transmission losses hence the dispersive properties of the material used in the nanostrip are selected accordingly. For lower THz frequency spectrum, the silver material can be selected with the conducting and dispersive properties as given in [51]. The antenna structure can be fabricated by utilizing the process explained in the literature [52–56] The metallic elements working as the feed and ground can be grown on SiO_2 substrate [54]. After fabricating the silicon in the shape of the proposed annular dielectric resonator, the chemical vapor deposition process can be utilized either for growing the graphene monolayer on it [55, 56] or by transferring approach [53, 54, 57]. A detailed discussion of the fabrication steps can be explored as reported in [52–56]. For obtaining the tunability in the antenna response, a graphene disk of thickness 0.34 *nm* having the properties defined by the parameters like chemical potential (μ_c), relaxation time (τ) at the room temperature $T = 300K$ is placed at the top of the silicon DR. The antenna structure is numerically analyzed and implemented using CST microwave studio. The optimized dimensions of antennas are mentioned in the caption of Fig. 1.

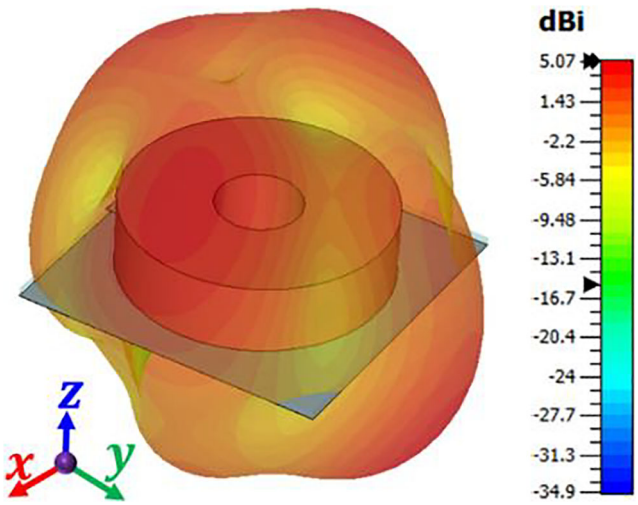

Fig. 6 3D radiation pattern of tunable DRA at frequency 4.104 THz

3 Results and Discussion

For understanding of antenna operation, two structures are implemented and analyzed; one without and another with graphene disk at the top of the silicon DR. Figure 2 shows the frequency response of S_{11} parameter and impedance of these both the antennas. The DRA without graphene disk at its top has the resonance at 4.088 THz. This antenna has the null-reactive impedance and peak of its real part at the resonant frequency. Placing the graphene disk with properties $\mu_c = 0\ eV$ and $\tau = 1ps$ at $T = 300K$ shifts the resonant frequency and frequency response in the forward direction. After placing the graphene disk at the top of the antenna, the new resonance frequency of the antenna becomes 4.104 THz. The shift in the resonant frequency after placing the graphene disk can be attributed to change in the material profile and medium properties at the interface of silicon DR and graphene boundaries. Also, this indicates that changing the electrical properties of the material placed at the top of the DR can tune the antenna response. Also, it is showing that graphene disk remains non-resonant over the operating frequency. Moreover, the shift in the resonant frequency reveals that addition of graphene ring only adds the value in the inductive and

Table 1 Performance of the antenna with and without graphene ring

Antenna	Operating mode	Resonant frequency (THz)	10 dB impedance bandwidth (GHz)	Gain (dBi)	Radiation efficiency (%)
DRA	$HEM_{41\delta}$	4.088	68	3.81	75
DRA+ Graphene disk	$HEM_{41\delta}$	4.104	67	3.79	72

capacitive part of impedance which can be realized as the parallel tank circuit using circuit theory approach [20]. It can be noticed that the impedance bandwidth of antenna remains approximately same in both the cases. The radiation mechanism of the proposed tunable DRA with graphene disk can be understood by observing the electric (E) and magnetic (H) field distribution. The field distribution is shown in Fig. 3 which shows the generation of hybrid modes. In Fig. 3a–e, there are eight vertical quadruple of E−field in the DR. Also, the H−field distribution shown in Fig. 3f–h shows that the vertical electrical quadruples are surrounded by the horizontal magnetic rings. Thus, it can be concluded that there is the generation of four vertical electric dipole in the annular DR. Thus, there are four half-wave variation along the azimuth angle. Also, there is single half-wave variation of field along the radius of the resonator. The partial variation of field can be considered along the height of the DR. Thus, the antenna operates with $HEM_{41\delta}$ mode. Here, the indices in suffix are showing the variation along azimuth, radial and height of the DR. The field variation is corresponding to the modal field analysis reported in the literature [50, 58]. Figure 4 shows the plot of gain and radiation efficiency. The antenna provides the gain and radiation efficiency more than 3 dBi and 72%, respectively over the operating passband.

Figure 5 shows the radiation pattern of tunable DRA at resonant frequency in all the principal planes. The separation between the co- and cross-polarized component of the radiated far-field is more than 60 dB which shows a good signal detection capability of antenna at receiver. Also, the front-to-back ratio of antenna is sufficiently large that enables to provide the high directivity around 5.07 dBi denoted by the 3D radiation pattern plot shown in Fig. 6.

The performance of both the antennas with and without graphene disk is reported in Table 1. The antenna operates with fourth order hybrid mode and provides high gain and radiation efficiency at the resonant frequency. The gain and radiation efficiency of the antenna is slightly reduced in the case of graphene disk is placed at the top of the DR. This may be due to losses occurred at the interface of the silicon dielectric and graphene disk.

4 Antenna Performance Analysis

A parametric study is carried out to know the effect of variation in physical parameters of proposed tunable DRA (DRA with graphene disk) on its response. The main parameters of antenna are inner and outer radius, r_i and r_o, respectively and height of the DR. These parameters are varied and effect is reported in Fig. 7. The outer radius of DR can be selected to operate at any frequency as shown in Fig. 7a. The inner radius plays an important role in the impedance matching. The appropriate selection of r_i provides good impedance matching as shown in Fig. 7b. The variation in r_i changes the power coupled to the DR from feedline which affects the impedance matching severely. Here, the proposed antenna operates with δ variation along the height of the DR. So, it can be concluded that the variation in height will affect the impedance matching and resonant frequency accordingly. The effect of varying the height on antenna response is mentioned in Fig. 7c. It can be observed in the plot that the impedance bandwidth is varied by lowering the reflection coefficient in the lower frequency region. Lowering the reflection coefficient confirms about the operation of antenna with the multiple operating modes. Thus, the antenna response can be set either with the multiple

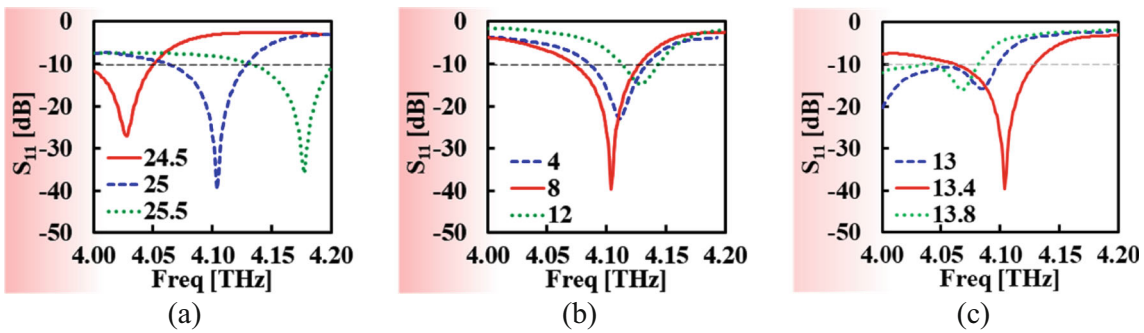

Fig. 7 The frequency response of tunable DRA for variable **a** r_o, **b** r_i and **c** h

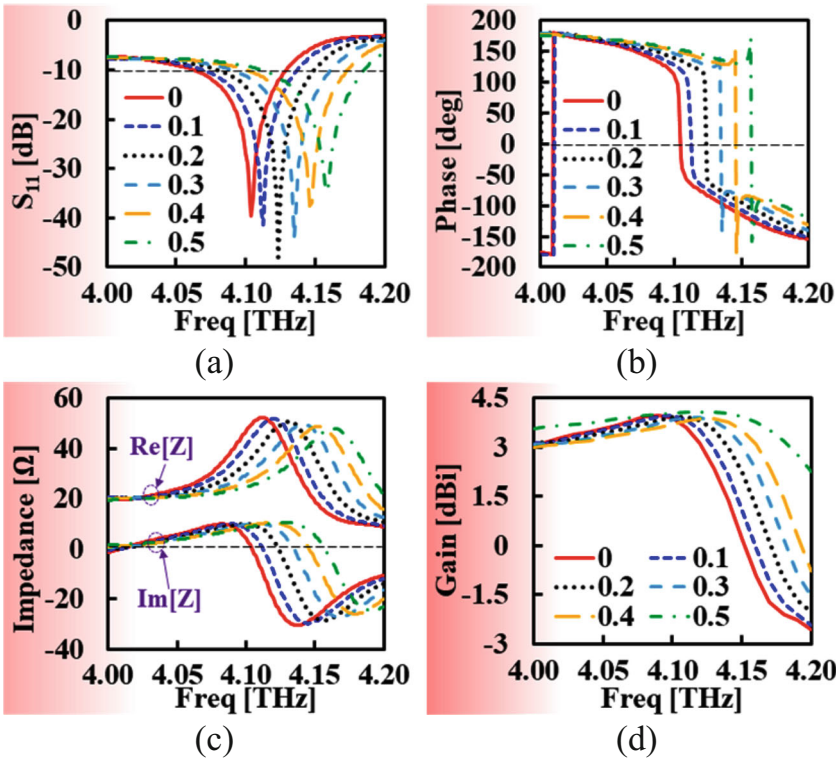

Fig. 8 Tuning of frequency response of **a** magnitude and **b** phase of S_{11}-parameter **c** impedance and **d** gain with $\mu_c\ (eV)$ $(T = 300K, \tau = 1ps)$

operating modes for providing the wide operating impedance bandwidth or with the single mode for providing narrowband frequency response with high selectivity. Moreover, the antenna response with and without graphene disk varies with the small change, hence the parametric variation of the antenna without graphene disk provides the variation in antenna

Table 2 Comparison with the other THz antennas

Category	Ref	Antenna	10 dB Impedance bandwidth (THz)	Gain (dBi)	RE (%)	Size (λ^3)	Tunability
1	[4]	Metallic patch	0.3 – 9.3	9.5	0 – 80	5.92 × 7.9 × 0.6	No
	[5]	Metallic patch	0.46 – 5.46	12	0 – 80	9.6 × 12.8 × 1.3	No
	[6]	Metallic patch	0.7 – 0.85	3.502	55.88	2.6 × 2.6 × 0.5	No
	[7]	Metamaterial cavity with reflector	0.47 – 0.65	10	–	0.86 × 0.56 × 0.112	No
	[8]	Metamaterial loaded patch	1.053 – 1.141	3.57	–	0.7 × 0.77 × 0.04	No
	[9]	Yagi-Uda with grating	1.84 – 2.42	3.9	100	0.7 × 0.64 × 0.007	No
	[10]	Patch with photonic crystal and FSS	0.5 – 0.7	7.3	–	1.2 × 1.2 × 0.55	No
2	[12]	Graphene patch	0.48 – 0.6	–	50	1 × 1 × 0.05	Yes
	[13]	Graphene Patch	0.55 – 0.58	–	40	1 × 1 × 0.05	Yes
	[18]	Y-shaped graphene patch	0.42 – 0.48	0.13	24	0.6 × 0.7 × 0.1	No
	[21]	Graphene stack	1.35 – 1.5	–	90	1 × 1 × 0.05	–
	[23]	Graphene dipole	0.9 – 1	–	21	0.64 × 0.38 × 0.13	Yes
	[24]	DR coupled to graphene radiator	2 – 3	7	70	1.7 × 1 × 1.05	–
	[25]	Graphene nano-ribbon radiator	0.924 – 1.2	2	44	1 × 1 × 0.1	Yes
	[26]	Graphene nano-ribbon radiator	0.64 – 0.82	–	26	1 × 1 × 0.64	Yes
3	[27]	Metallic patch with graphene ribbons	4.76 – 19	6.4	80	0.95 × 0.8 × 0.075	Yes
	[29]	Metallic ring with graphene	1.10	1	–	0.6 × 0.6 × 0.003	Yes
	[30]	Graphene with metamaterial	1.7	–	60	0.28 × 0.06 × 0.15	Yes
	[31]	Yagi antenna with graphene	0.97 – 1.12	8.24	–	0.77 × 0.55 × 0.0035	Yes
	[32]	Patch with graphene load	0.95 – 1.05	11	78	1.26 × 1.26 × 0.65	Yes
	This Antenna	Graphene disk loaded DR	4.0629 – 4.1299	3.8	72 – 75	0.81 × 0.81 × 0.18	Yes

–*not reported,* RE–radiation efficiency

response in the similar manner as with graphene disk (as mentioned in Fig. 2). For brevity, the parametric variation of the antenna without graphene disk is not reported in the manuscript.

5 Tuning of Frequency Response

The top of the silicon DR is coated with the monolayer graphene material having thickness 0.34 *nm*. The purpose of coating of silicon DR by graphene material is to utilize its property that its surface conductivity can be tuned by applying an external electrostatic DC field [59–61]. Figure 8 shows the antenna response with variation in μ_c. Figure 8a, b shows the variation in magnitude and phase of the S_{11} parameter response of antenna. It can be observed in the plots that the resonant frequency and covered 10 dB impedance bandwidth can be steered over the frequency with the variation in μ_c. The phase of S_{11} parameter at resonant frequency varies linearly with each value of μ_c confirming that the radiation properties of antenna remain same after changing the value of chemical potential of graphene. Figure 8c shows the impedance plot of antenna for different values of μ_c. This confirms about the shift in resonant frequency of the operating mode with the variation in μ_c. Also, linear plot shows the antenna operation with single mode. The gain plot is reported in Fig. 8d showing that the peak of gain is also shifting in correlation with the operating passband, as expected.

Table 2 shows the comparison of the proposed antenna with other THz antennas existing in the literature. The comparison table shows that many antennas of first category can provide high gain [4, 5, 7, 10] and radiation efficiency [4, 5, 9], but their response cannot be tuned like the proposed tunable DRA. Also, they have the limitation of large size in comparison to the proposed antenna. Also, it is still a question in the case of metallic antennas that whether practically they are this much efficient at higher frequencies or not [4, 5]. In the second category, most of the antennas provide the low value of gain and radiation efficiency in comparison to the proposed antenna. Some antennas provide high gain [24] and radiation efficiency [21] but they have large size in comparison. In the similar manner, some antennas in the third category can provide the tunability with high gain [31] and radiation efficiency [31, 32], but they have the limitation of size and other performance parameters. Overall, it can be concluded that the proposed antenna can replace many others in terms of gain, radiatin efficiency, size and tunability. Also, the proposed antenna can avoid the fabrication complexities in comparison to other implemented by utilizing the FSS and metamaterial [10, 30, 32]. Furthermore, in most of antennas of second and third categories, the tunability is achieved but the performance characteristics and frequency response is not preserved with the variation in the chemical potential of graphene [16, 31–34]. The proposed antenna offers the capability over such antennas and preserves its frequency response for all values of μ_c.

6 Conclusion

A tunable DRA is numerically analyzed and implemented for THz applications. The frequency response of antenna has been tuned by changing the chemical potential of graphene disk placed at the top of the DR. The parametric variation in the physical dimensions of antenna reveals that the antenna response can be tuned either with the single or multiple operating modes. The aspect ratio of DR and other parameters have been selected to suppress the lower order modes and to operate with the single higher order hybrid electromagnetic mode. Placing the graphene disk at the top of the antenna does not affect the antenna operation. The antenna response can be preserved over a wide range of chemical potential of graphene. The THz DRA without graphene disk at its top provides the gain and radiation efficiency around 3.81 dBi and 75%, respectively. The performance indices are slightly deteriorated with insignificant amount in the case of proposed tunable THz DRA with graphene disk. The proposed antenna provides gain around 3.79 dBi and radiation efficiency 72 − 75% with the tunable frequency response at THz frequency.

References

1. Akyildiz IF, Jornet JM, Han C (2014) Terahertz band: next frontier for wireless communications. Phys Commun 12:16–32. https://doi.org/10.1016/j.phycom.2014.01.006
2. Varshney G, Gotra S, Kaur J, Pandey VS, Yaduvanshi RS (2019) Obtaining the circular polarization in a nano-dielectric resonator antenna for photonics applications. Semicond Sci Technol 34(7): 07LT01. https://doi.org/10.1088/1361-6641/ab1fd1
3. Varshney G (2020) Ultra-wideband antenna using graphite disk resonator for THz. Superlattices Microstruct. https://doi.org/10.1016/j.spmi.2020.106480
4. Singhal S (2019) Ultrawideband elliptical microstrip antenna for terahertz applications. Microw Opt Technol Lett 61(10):2366–2373. https://doi.org/10.1002/mop.31910
5. Singhal S (2019) Elliptical ring terahertz fractal antenna. Optik (Stuttg) 194(May):163129. https://doi.org/10.1016/j.ijleo.2019.163129
6. Sharma A, Singh G (2009) Rectangular microstirp patch antenna design at THz frequency for short distance wireless communication systems. J Infrared Millimeter Terahertz Waves 30(1):1–7. https://doi.org/10.1007/s10762-008-9416-z
7. Sadeghzadeh RA, Zarrabi FB (2016) Metamaterial Fabry-Perot cavity implementation for gain and bandwidth enhancement of THz dipole antenna. Optik (Stuttg) 127(13):5181–5185. https://doi.org/10.1016/j.ijleo.2016.02.072
8. Denizhan Sirmaci Y, Akin CK, Sabah C (2016) Fishnet based metamaterial loaded THz patch antenna. Opt Quant Electron 48(2):1–10. https://doi.org/10.1007/s11082-016-0449-6

9. Poorgholam-Khanjari S, Zarrabi FB, Jarchi S (2020) Compact and wide-band Quasi Yagi-Uda antenna based on periodic grating ground and coupling method in terahertz regime. Optik (Stuttg) 203(December 2019):163990. https://doi.org/10.1016/j.ijleo.2019.163990
10. Nejati A, Sadeghzadeh RA, Geran F (2014) Effect of photonic crystal and frequency selective surface implementation on gain enhancement in the microstrip patch antenna at terahertz frequency. Phys B Condens Matter 449:113–120. https://doi.org/10.1016/j.physb.2014.05.014
11. Malheiros-Silveira GN, Wiederhecker GS, Hernández-Figueroa HE (2013) Dielectric resonator antenna for applications in nanophotonics. Opt Express 21(1):1234. https://doi.org/10.1364/oe.21.001234
12. Naghdehforushha SA, Moradi G (2018) High directivity plasmonic graphene-based patch array antennas with tunable THz band communications. Optik (Stuttg) 168:440–445. https://doi.org/10.1016/j.ijleo.2018.04.104
13. Naghdehforushha SA, Moradi G (2018) Plasmonic patch antenna based on graphene with tunable terahertz band communications. Optik (Stuttg) 158:617–622. https://doi.org/10.1016/j.ijleo.2017.12.088
14. Dong Y, Liu P, Yu D, Li G, Tao F (2016) Dual-band reconfigurable terahertz patch antenna with graphene-stack-based backing cavity. IEEE Antennas Wirel Propag Lett 15:1541–1544. https://doi.org/10.1109/LAWP.2016.2533018
15. Varshney G, Verma A, Pandey VS, Yaduvanshi RS, Bala R (2018) A proximity coupleld wideband graphene antenna with the generation of higher order TM modes for THz application. Opt Mater. Elsevier, 85:456–463
16. Naghdehforushha SA, Moradi G (2019) An improved method to null-fill H-plane radiation pattern of graphene patch THz antenna utilizing branch feeding microstrip line. Optik (Stuttg) 181(November 2018):21–27. https://doi.org/10.1016/j.ijleo.2018.11.155
17. Kiani N, Tavakkol Hamedani F, Rezaei P, Jafari Chashmi M, Danaie M (2020) Polarization controling approach in reconfigurable microstrip graphene-based antenna. Optik (Stuttg) 203(September 2019):163942. https://doi.org/10.1016/j.ijleo.2019.163942
18. Jafari Chashmi M, Rezaei P, Kiani N (2020) Y-shaped graphene-based antenna with switchable circular polarization. Optik (Stuttg) 200(August 2019):163321. https://doi.org/10.1016/j.ijleo.2019.163321
19. Varshney G, Gotra S, Pandey VS, Yaduvanshi RS (2019) Proximity-coupled two-port multi-input-multi-output graphene antenna with pattern diversity for THz applications. Nano Commun Netw 21:100246. https://doi.org/10.1016/j.nancom.2019.05.003
20. Varshney G (2020) Reconfigurable graphene antenna for THz applications: a mode conversion approach. Nanotechnology 31(13):135208. https://doi.org/10.1088/1361-6528/ab60cc
21. Naghdehforushha SA, Moradi G (2019) High radiation efficiency of coupled plasmonic graphene-based THz patch antenna utilizing strip slot ground plane removal. Optik (Stuttg) 182:1082–1087. https://doi.org/10.1016/j.ijleo.2019.01.099
22. Bala R, Marwaha A (2016) Characterization of graphene for performance enhancement of patch antenna in THz region. Optik (Stuttg). 127(4):2089–2093. https://doi.org/10.1016/j.ijleo.2015.11.029
23. Chashmi MJ, Rezaei P, Kiani N (2019) Reconfigurable graphene-based V-shaped dipole antenna: From quasi-isotropic to directional radiation pattern. Optik (Stuttg) 184(February):421–427. https://doi.org/10.1016/j.ijleo.2019.04.125
24. Hosseininejad SE et al (2018) Terahertz dielectric resonator antenna coupled to graphene plasmonic dipole. EuCAP. https://doi.org/10.1049/cp.2018.1041
25. Nickpay MR, Danaie M, Shahzadi A (2019) Wideband rectangular double-ring nanoribbon graphene-based antenna for terahertz communications. IETE J Res:1–10. https://doi.org/10.1080/03772063.2019.1661801
26. Naghdehforushha SA, Moradi G (2018) Design of plasmonic rectangular ribbon antenna based on graphene for terahertz band communication. IET Microwaves Antennas Propag 12(5):804–807. https://doi.org/10.1049/iet-map.2017.0678
27. Sharma T, Varshney G, Vashishath RSYM (2020) Obtaining the tunable band-notch in ultrawideband THz antenna using graphene nanoribbons. Opt Eng 59(4):047103–1–047103–11. https://doi.org/10.1117/1.OE.59.4.047103
28. Novin SN, Zarrabi FB, Bazgir M, Heydari S, Ebrahimi S (2019) Field enhancement in metamaterial split ring resonator aperture nano-antenna with spherical nano-particle arrangement. Silicon 11(1):293–300. https://doi.org/10.1007/s12633-018-9854-8
29. Cheng X, Yao Y, Qu S-W, Wu Y, Yu J, Chen X (2016) Circular beam-reconfigurable antenna base on graphene-metal hybrid circular beam-reconfigurable antenna base on graphene-metal hybrid. Electron Lett 52(7):494–496. https://doi.org/10.1021/nl803316h
30. Amanatiadis SA, Karamanos TD, Kantartzis NV (2017) Radiation efficiency enhancement of graphene THz antennas utilizing metamaterial substrates. IEEE Antennas Wirel Propag Lett 16:2054–2057. https://doi.org/10.1109/LAWP.2017.2695521
31. Zarrabi FB, Seyedsharbaty MM, Ahmed Z, Arezoomand AS, Heydari S (2017) Wide band yagi antenna for terahertz application with graphene control. Optik (Stuttg) 140:866–872. https://doi.org/10.1016/j.ijleo.2017.05.009
32. Seyedsharbaty MM, Sadeghzadeh RA (2017) Antenna gain enhancement by using metamaterial radome at THz band with reconfigurable characteristics based on graphene load. Opt Quant Electron 49(6):1–13. https://doi.org/10.1007/s11082-017-1052-1
33. Kazemi F (2020) Dual band compact fractal THz antenna based on CRLH-TL and graphene loads. Optik (Stuttg) 206(December 2019):164369. https://doi.org/10.1016/j.ijleo.2020.164369
34. Samanta G, Mitra D (2018) Wideband THz antenna using graphene based tunable circular reactive impedance substrate. Optik (Stuttg) 158:1080–1087. https://doi.org/10.1016/j.ijleo.2017.12.197
35. Walther M, Cooke DG, Sherstan C, Hajar M, Freeman MR, Hegmann FA (2007) Terahertz conductivity of thin gold films at the metal-insulator percolation transition. Phys Rev B Condens Matter Mater Phys 76(12):1–9. https://doi.org/10.1103/PhysRevB.76.125408
36. Chen J-X, Shi J, Bao Z-H, Xue Q (2011) Tunable and switchable bandpass filters using slot-line resonators. Prog Electromagn Res 111:25–41. https://doi.org/10.2528/Pier10100808
37. Ju L, Geng B, Horng J, Girit C, Martin M, Hao Z, Bechtel HA, Liang X, Zettl A, Shen YR, Wang F (2011) Graphene plasmonics for tunable terahertz metamaterials. Nat Nanotechnol 6(10):630–634. https://doi.org/10.1038/nnano.2011.146
38. Khan M, Tahir MN, Adil SF, Khan HU, Siddiqui MRH, al-warthan AA, Tremel W (2015) Graphene based metal and metal oxide nanocomposites: synthesis, properties and their applications. J Mater Chem A 3(37):18753–18808. https://doi.org/10.1039/c5ta02240a
39. Sensale-rodriguez B, Member S, Yan R, Jena D, Xing HG (2013) Graphene for reconfigurable THz optoelectronics. Proc IEEE 101(7):1705–1716
40. Wang R, Ren XG, Yan Z, Jiang LJ, Sha WEI, Shan GC (2019) Graphene based functional devices: a short review. Front Phys 14(1). https://doi.org/10.1007/s11467-018-0859-y
41. Gale JD et al (2012) The rise of graphene. Rev Mod Phys 58(1):710–734. https://doi.org/10.1016/j.jmps.2010.02.008
42. Low T, Avouris P (2014) Graphene plasmonics for terahertz to mid-infrared applications. ACS Nano 8(2):1086–1101. https://doi.org/10.1021/nn406627u

43. Ghorbanzadeh Ahangari M, Salmankhani A, Imani AH, Shahab N, Hamed Mashhadzadeh A (2019) Density functional theory study on the mechanical properties and interlayer interactions of multilayer graphene: carbonic, silicon-carbide and silicene graphene-like structures. Silicon 11(3):1235–1246. https://doi.org/10.1007/s12633-018-9885-1
44. Gomez-Diaz JS, Moldovan C, Capdevila S, Romeu J, Bernard LS, Magrez A, Ionescu AM, Perruisseau-Carrier J (2015) Self-biased reconfigurable graphene stacks for terahertz plasmonics. Nat Commun 6:1–8. https://doi.org/10.1038/ncomms7334
45. Verma A, Prakash A, Tripathi R (2017) Comparative study of a surface plasmon resonance biosensor based on metamaterial and graphene. Silicon 9(3):309–320. https://doi.org/10.1007/s12633-016-9455-3
46. Varshney G, Pandey VS, Yaduvanshi RS (2018) Axial ratio bandwidth enhancement of a circularly polarized rectangular dielectric resonator antenna. Int J Microw Wirel Technol 10(8):984–990. https://doi.org/10.1017/s1759078718000764
47. Gotra S, Varshney G, Pandey VS, Yaduvanshi RS (2019) Super-wideband multi-input–multi-output dielectric resonator antenna. IET Microwaves Antennas Propag 14(1):21–27. https://doi.org/10.1016/j.jallcom.2008.03.118
48. Withayachumnankul W et al (2013) Dielectric resonator nanoantennas at visible frequencies. Opt Express 21(1):1344. https://doi.org/10.1364/oe.21.001344
49. Gotra S, Varshney G, Yaduvanshi RS, Pandey VS (2019) Dual-band circular polarisation generation technique with the miniaturisation of a rectangular dielectric resonator antenna. IET Microwaves, Antennas Propag:Accepted. https://doi.org/10.1049/iet-map.2019.0030
50. Varshney G, Gotra S, Pandey VS, Yaduvanshi RS (2018) Inverted-sigmoid shaped multiband dielectric resonator antenna with dual-band circular polarization. IEEE Trans Antennas Propagat 66(4):2067–2072. https://doi.org/10.1109/TAP.2018.2800799
51. Michalski KA, Zheng D (1992) Analysis of microstrip resonators of arbitrary shape. IEEE Trans Microw Theory Tech 40(1):112–119. https://doi.org/10.1109/22.108330
52. Li X, Cai W, An J, Kim S, Nah J, Yang D, Piner R, Velamakanni A, Jung I, Tutuc E, Banerjee SK, Colombo L, Ruoff RS (2009) Large-area synthesis of high-quality and uniform graphene films on copper foils. Science (80-) 324(5932):1312–1314. https://doi.org/10.1126/science.1171245
53. Kim KS, Zhao Y, Jang H, Lee SY, Kim JM, Kim KS, Ahn JH, Kim P, Choi JY, Hong BH (2009) Large-scale pattern growth of graphene films for stretchable transparent electrodes. Nature 457(7230):706–710. https://doi.org/10.1038/nature07719
54. Liu W et al (2018) Graphene-enabled electrically controlled terahertz meta-lens. Photonics Res 6(7):703. https://doi.org/10.1364/prj.6.000703
55. Tai L, Zhu D, Liu X, Yang T, Wang L, Wang R, Jiang S, Chen Z, Xu Z, Li X (2018) Direct growth of graphene on silicon by metal-free chemical vapor deposition. Nano-Micro Lett 10(2):1–9. https://doi.org/10.1007/s40820-017-0173-1
56. Xiang P, Wang G, Yang S, Liu Z, Zheng L, Li J, Xu A, Zhao M, Zhu W, Guo Q, Chen D (2019) In situ synthesis of monolayer graphene on silicon for near-infrared photodetectors. RSC Adv 9(64):37512–37517. https://doi.org/10.1039/c9ra06792b
57. Chen XD, Liu ZB, Zheng CY, Xing F, Yan XQ, Chen Y, Tian JG (2013) High-quality and efficient transfer of large-area graphene films onto different substrates. Carbon N Y 56:271–278. https://doi.org/10.1016/j.carbon.2013.01.011
58. Kajfez D, Glisson AW, James J (1984) Computed modal field distributions for isolated dielectric resonators. IEEE Trans Microw Theory Tech 32(12):1609–1616. https://doi.org/10.1109/TMTT.1984.1132900
59. Hanson GW (2008) Dyadic green's functions for an anisotropic, non-local model of biased graphene. IEEE Trans Antennas Propag 56(3):747–757. https://doi.org/10.1109/TAP.2008.917005
60. Geim AK, Novoselov KS (2007) The rise of graphene. Nat Mater 6(3):183–191. https://doi.org/10.1038/nmat1849
61. Varshney G, Gotra S, Pandey VS, Yaduvanshi RS (2019) Proximity-coupled Graphene-patch-based tunable single−/dual-band notch filter for THz applications J Electron Mater. Springer, 48(8):4818–4829. https://doi.org/10.1007/s11664-019-07274-8